THE ASTROPHYSICAL JOURNAL, 311:360–370, 1986 December 1

INFRARED REFLECTION NEBULAE IN ORION MOLECULAR CLOUD 2

YVONNE PENDLETON[1, 2] AND M. W. WERNER[1]
NASA/Ames Research Center, Moffett Field, California
R. CAPPS[1]
University of Hawaii
AND
D. LESTER
University of Texas, Austin
Received 1986 March 11; accepted 1986 May 12

ABSTRACT

New observations of Orion Molecular Cloud 2 have been made from 1 to 100 μm using the NASA Infrared Telescope Facility and the Kuiper Airborne Observatory. An extensive program of polarimetry, photometry, and spectrophotometry has shown that the extended emission regions associated with two of the previously known near-infrared sources, IRS 1 and IRS 4, are infrared reflection nebulae, and that the compact sources IRS 1 and IRS 4 are the main luminosity sources in the cloud. The constraints from the far-infrared observations and an analysis of the scattered light from the IRS 1 nebula show that OMC-2/IRS 1 can be characterized by $L \leq 500\ L_\odot$ and $T \approx 1000$ K. The near-infrared (1–5 μm) albedo of the grains in the IRS 1 nebula is greater than 0.08.

Subject headings: infrared: sources — interstellar: grains — interstellar: molecules — nebulae: reflection — polarization

I. INTRODUCTION

Infrared polarimetry can be an effective tool in an investigation of dust-embedded prestellar objects and their surrounding medium. Polarimetry has shown in many instances that the extended near-infrared emission in regions of star formation is scattered light, since it shows high polarization that can be produced only by scattering (Tokunaga, Lebofsky, and Rieke 1981; Werner, Dinerstein, and Capps 1983; Joyce and Simon 1986). In regions that are polarized by scattering, the orientations of the electric vectors clearly identify the luminosity sources. The scattering provides a second look at the illuminating object, through the reflected light, which can be complementary to direct line-of-sight observations of the source.

We have used infrared polarimetry to probe the infrared cluster in Orion Molecular Cloud 2 (OMC-2). OMC-2 is a 2.5 × 3.0 region of infrared and molecular emission located about 12′ northeast of the Trapezium. Gatley *et al.* (1974) have shown that, at 2.2 μm, OMC-2 contains five point sources plus extended emission. We use their nomenclature (IRS 1, IRS 2, etc.) to identify the point sources. The redness of these objects, the absence of optical counterparts, and their association with molecular emission peaks (Batrla *et al.* 1983; Kutner, Evans, and Tucker 1976) suggest that this is a region of current star formation. Thronson *et al.* (1978) have measured a total luminosity for OMC-2 in the far-infrared of 2100 $L_\odot$ into a 3.5 beam. The absence of ionizing radiation and the low luminosity imply that if stars are forming in OMC-2, they are less massive than those forming in the core of OMC-1. In this paper we present new observations of OMC-2 which include photometry, spectrophotometry, and polarimetry in the 1–30 μm region as well as 50 μm and 100 μm photometric maps. We have determined that the extended emission in the region of OMC-2/IRS 1 is a particularly good example of an infrared reflection nebula. We have also identified, in the near-infrared, a second region of high polarization and a previously unresolved double source structure in OMC-2/IRS 4. The far-infrared measurements have allowed us to identify OMC-2/IRS 1 and OMC-2/IRS 4 as the primary luminosity sources within the cluster, to determine their luminosities, and to infer the dust optical depths and grain temperatures. The total luminosity inferred from the far-infrared measurements provides an important additional constraint on the interpretation of the near-infrared data; the near- and far-infrared observations together set new constraints on the properties of the embedded sources in this region.

[1] Visiting Astronomer at the Infrared Telescope Facility, which is operated by the University of Hawaii under contract from the National Aeronautics and Space Administration.

[2] Also Board of Studies in Astronomy and Astrophysics, University of California, Santa Cruz.

II. OBSERVATIONS

a) *Near-infrared*

The 1–30 μm observations were made at the NASA Infrared Telescope Facility from 1982 October to 1984 December, using the facility instruments. Broad-band photometry, one-dimensional scans, or comprehensive mapping were done at 1.25 μm ($\Delta\lambda = 0.3$), 1.65 μm ($\Delta\lambda = 0.35$), 2.2 μm ($\Delta\lambda = 0.42$), 3.1 μm ($\Delta\lambda = 0.1$), 3.8 μm ($\Delta\lambda = 0.67$), and 4.8 μm ($\Delta\lambda = 0.57$), with either a 6″ or 4″ beam, using the IRTF InSb system. The chopper spacing was between 35″ and 45″ north-south for the IRS 1 measurements and 60″ east-west for the IRS 4 region. Spectra were obtained in the $2.8 \leq \lambda \leq 3.7$ μm range with resolution of 2%. The 8.7 μm ($\Delta\lambda = 1.2$), 9.7 μm ($\Delta\lambda = 1.2$), 10.3 μm ($\Delta\lambda = 5.2$), 12.5 μm ($\Delta\lambda = 1.2$), 20 μm ($\Delta\lambda = 9$), and 30 μm ($\Delta\lambda = 8$) photometry was done with the IRTF Ge:Ga bolometer, using 4″ and 8″ beams. The chopper spacing for the 9–30 μm observations was 30″ east-west. Absolute fluxes were determined by using standard calibration stars with cali-

bration uncertainties of ~10% in the 1–5 μm range and ~25% in the 9–30 μm range.

Polarization measurements were made in the 2.2 μm and 3.8 μm broad-band filters using a rotating wire grid, as described in Werner, Dinerstein, and Capps (1983). The polarization results were corrected for instrumental polarization (typically 2% or less) by subtracting the net polarization values measured for several intrinsically unpolarized stars. Absolute position angles were determined by reference to the Becklin-Neugebauer source (BN) for which the position angle is known to be 117° measured east from north (Dyck and Lonsdale 1981, and references therein).

We determined the positions of IRS 1 and of both components of IRS 4 relative to that of IRS 3, which is known to be located at $\alpha(1950) = 5^h32^m59^s.1 \pm 0^s.1$, $\delta(1950) = -5°12'10'' \pm 1''$ (Gatley *et al.* 1974). Positions and offsets for IRS 1 and IRS 4 relative to IRS 3 are given in Table 1.

b) *Far-infrared*

Photometric maps were made with a 30″ FWHM beam at 50 μm ($\Delta\lambda = 25$ μm) and 100 μm ($\Delta\lambda = 50$ μm) in 1984 February from the Kuiper Airborne Observatory at an altitude of 12.5 km. The University of Texas six-channel photometer (Wilking *et al.* 1984) mounted at the Cassegrain focus of the KAO 91 cm telescope allowed measurements in both passbands to be made at each of three positions on the sky simultaneously. The instrumentation is similar to that described by Harvey (1979). The maps were made by offsetting in the KAO focal plane from a guide star located at $\alpha(1950) = 5^h33^m06^s.4$, $\delta(1950) = -5°08'14''$. The positional uncertainties are ±5″. Position steps of 20″.3 were taken in the north-south direction and 10″.2 in the east-west direction until an area of 2′.5 × 3′.0 was covered; the area mapped is outlined by the dashed line in Figure 1. The chopper spacing was 5′ in azimuth, which was close to east-west for these observations. The far-infrared observations were calibrated relative to S140-IR (Harvey, Wilking, and Joy 1984). The calibration uncertainty is ~20%.

III. RESULTS

a) *Far-infrared Maps*

Figures 1 and 2 show the flux contour maps at 50 and 100 μm respectively. The near-infrared source positions for IRS 1, IRS 2, IRS 3, and IRS 4, which we determined from 2.2 μm photometry, and the position of IRS 5, determined by Gatley *et al.* (1974), are indicated on these maps. The 50 μm map shows two peaks, one coincident with the position of IRS 4 and a second, less pronounced peak coincident with the position of IRS 1, as well as a slight amount of emission extended in the direction of IRS 3. The 100 μm map is dominated by the peak at IRS 4 and shows emission extended toward IRS 1, which does not appear as a distinct peak. The spatial distribution and extent of the extended emission seen at 100 μm is similar to that seen at 2.2 μm by Gatley *et al.* (1974), as shown in Figure 2.

TABLE 1

ORION MOLECULAR CLOUD 2: SOURCE POSITIONS

INFRARED SOURCE	2.2 μm PEAK FLUX POSITION (1959) R.A. ± 0ˢ.1	Decl. ± 1″	OFFSET FROM IRS 3
IRS 1	$5^h32^m56^s.9$	−5°12′21″.3	33″.3 west, 11″.3 south
IRS 2	5 32 58.7	−5 11 18	6″ west, 52″ north
IRS 3	5 32 59.1	−5 12 10[a]	...
IRS 4-N	5 32 59.8	−5 11 26.1	9″.7 east, 43″.9 north
IRS 4-S	5 32 59.8	−5 11 30.1	9″.7 east, 39″.9 north

[a] Gatley *et al.* 1974.

The results of the infrared photometry and polarimetry are given in Table 2. The 50 μm flux densities into the 30″ beam are 530 Jy for IRS 4 and 185 Jy for IRS 1. The former result is consistent with the flux density of 570 Jy measured at 61 μm into an 18″ × 28″ beam that included IRS 4 and IRS 1 by Thronson *et al.* (1978). The far-infrared maps show that the region around IRS 3 does not emit strongly at 50 μm, so that the Thronson *et al.* (1978) measurement is dominated by flux from IRS 4. Color temperatures derived from the 50 and 100 μm data are between 35 and 50 K in both the IRS 1 and IRS 4 regions. Assuming that the emissivity falls as λ^{-1}, grain temperatures for these areas are between 30 and 40 K. Optical depths at 50 and 100 μm were derived from the grain temperature and the observed flux and show that both the IRS 1 and IRS 4 regions are optically thin. The peak optical depth at 100 μm toward IRS 1 is $\tau_{100} = 0.02$, which implies an average value for the visual extinction over the 30″ beam of $A_v \approx 15$, assuming $\tau_{UV}/\tau_{125} = 2000$ (Whitcomb *et al.* 1981) and an interstellar extinction law based on the results of Savage and Mathis (1979).

We measure a total flux of 5300 Jy at 100 μm and 715 Jy at 50 μm for the 2′.5 × 1′.8 area within the lowest contour on Figure 2. This implies a 40–150 μm luminosity of 900 $L_\odot$ for this area, assuming a distance of 500 pc. This far exceeds the near-infrared (1–20 μm) luminosity of ~100 $L_\odot$. IRS 1 and IRS 4 coincide with peaks in both 50 μm brightness and far-infrared color temperature. Therefore, we conclude that IRS 1 and IRS 4 are the primary luminosity sources in OMC-2, and that the far-infrared radiation is thermal emission from dust heated by these sources. The integrated flux into a 30″ beam at the peak position is 130 $L_\odot$ for IRS 1 and 400 $L_\odot$ for IRS 4. Thus, much of the luminosity of these sources is reradiated by the extended dust cloud. Our luminosity determination agrees satisfactorily with that of Thronson *et al.* (1978), who measured 2100 $L_\odot$ into a 3′.5 beam centered on OMC-2, using a ~9′ chopper throw.

b) *Near-infrared*

The photometry and polarimetry results are presented in Table 2. The near-infrared photometric results agree with those of Gatley *et al.* (1974). New observations of OMC-2/IRS 2 are presented in Table 2, although they are not discussed in the text.

i) *IRS 1*

We mapped the extended emission in the region between IRS 1 and IRS 3 at 2.2 and 3.8 μm, as shown in Figures 3 and 4, and found the emission to be highly polarized at both wavelengths (up to 31% at 3.8 μm). The contours in Figures 3 and 4 are logarithmic to emphasize the low-surface-brightness extended emission between the infrared peaks. The length of the heavy lines in Figures 3 and 4 indicates the percent polarization p, while the orientation of the dark lines displays the position angle of the maximum electric vector. The high polarization values of $6 \leq p \leq 23$ at 2.2 μm and $13 \leq p \leq 31$ at 3.8 μm suggests that scattering is responsible (Werner, Diner-

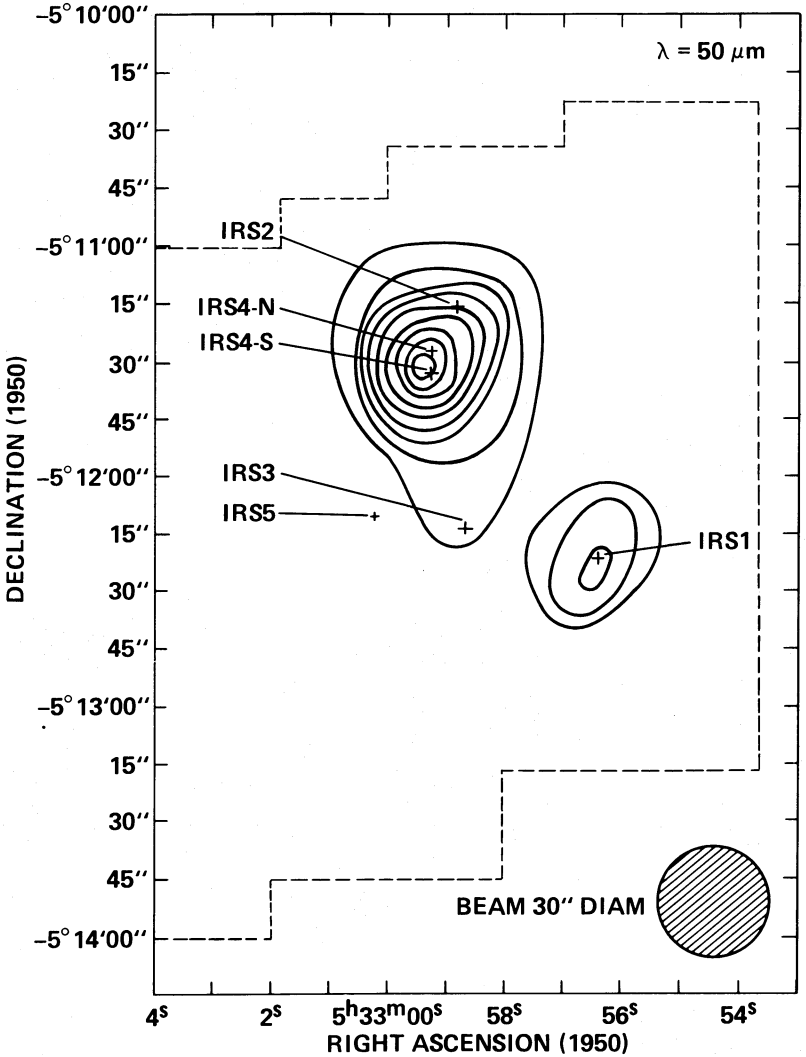

FIG. 1

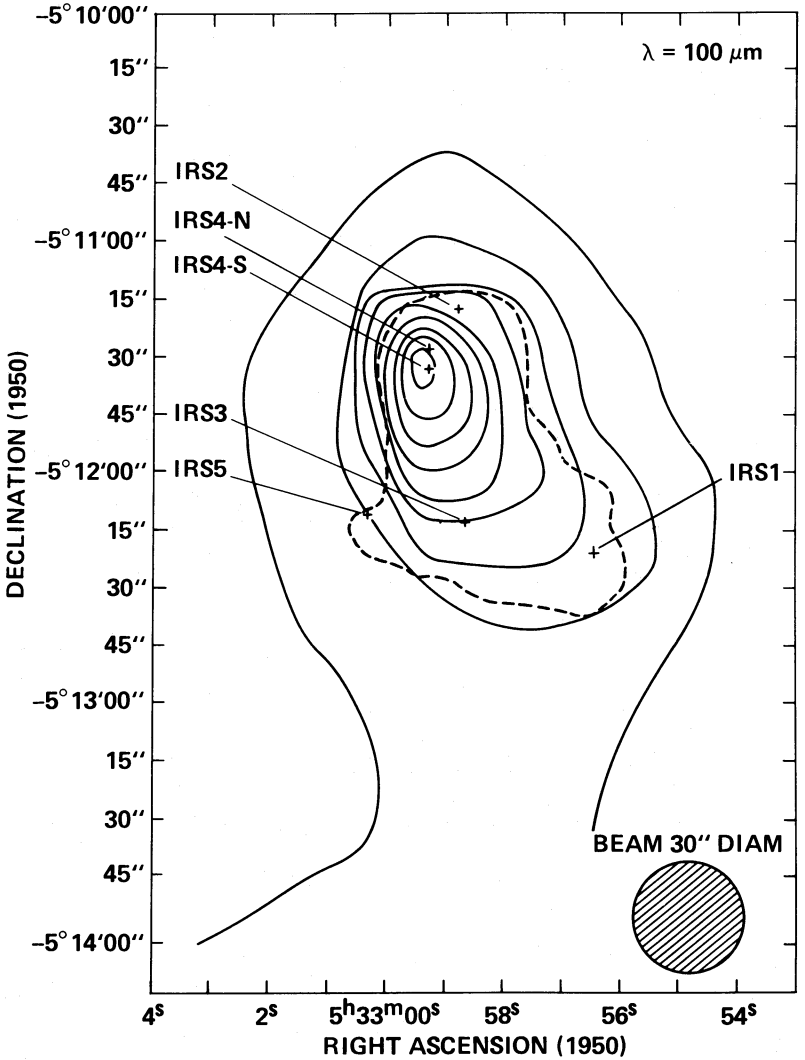

FIG. 2

FIG. 1.—50 μm map of the OMC-2 cluster made using a 30″ beam on a 20.″3 × 10.″2 grid. Contour levels are 0.1, 0.2, 0.3, 0.4, 0.5, 0.6, 0.7, 0.8, and 0.9 times the peak value of 530 Jy into a 30″ beam. The 2.2 μm positions of the near-infrared peaks are designated by the pluses. The 2.′5 × 3.′0 region mapped is outlined by the dashed contour.

FIG. 2.—100 μm map of the OMC-2 cluster made using a 30″ beam on a 20.″3 × 10.″2 grid. Contour levels are 0.1, 0.2, 0.3, 0.4, 0.5, 0.6, 0.7, 0.8, and 0.9 times the peak value of 1620 Jy into a 30″ beam. The 2.2 μm positions of the near infrared peaks are designated by the pluses. The dashed line is the lowest contour of the 2.2 μm flux measured by Gatley *et al.* (1974).

TABLE 2

OBSERVATIONS[a]

λ (μm)	IRS 1[b]	IRS 1 NEBULA[c] 5″[d]	8″[d]	14″[d]	IRS 4[b] South	North	IRS 3[c]	IRS 2[c]
Photometry: F_λ ($\times 10^{-18}$ W cm^{-2} μm^{-1})								
Near-infrared:								
1.25.....	0.2	0.7	0.8	0.3	1.6	0.1	1.5	0.1
1.65.....	1.5	3.4	3.5	1.4	7.1	0.3	13.8	0.7
2.2.....	7.1	5.6	5.6	2.4	10.4	1.4	41.8	2.3
3.05.....	1.8	0.9	0.7	0.3	4.1	0.3	33.2	3.3
3.8.....	17.8	2.4	2.0	1.1	6.8	5.0	86.2	11.9
4.8.....	25.3	1.5	0.9	0.8	5.8	6.2	98.3	19.7
8.7.....	...	...	...	...	3.5	1.0	...	...
9.7.....	...	...	...	...	3.2	0.78 ± 0.2	...	...
10.3.....	26.0	<0.4	...	...	3.4	1.2	51.4[e]	...
12.5.....	...	...	...	...	3.1 ± 0.4	1.4 ± 0.4	37.0[e]	...
20.....	30.0	<0.7	...	...	3.3	9.4	21.0[e]	...
30.....	...	...	...	...	...	21.0[f]	...	...
Far-infrared:								
50.....	20.0	...	...	...		60.0	...	...
100.....	15.0	...	...	...		50.0	...	...
Polarimetry								
p:								
2.2.....	<6%	7%	10%	23%	<6%	19%	...	...
3.8.....	<6	13	25	31	<6	25	<6%	...
θ:								
2.2.....	...	143°	141°	140°	...	89°	...	...
3.8.....	...	139	149	137	...	80	...	...

[a] Flux errors <10% unless indicated; polarimetry errors ± 2%; position angle uncertainties ± 3°; upper limits 3 σ.
[b] Beam size: near-infrared, 4″; far-infrared, 30″.
[c] Beam size: 6″, unless otherwise noted.
[d] Distance of point north and east of IRS 1.
[e] Beam size: 4″.
[f] We associate this flux with the position of IRS 4-N.

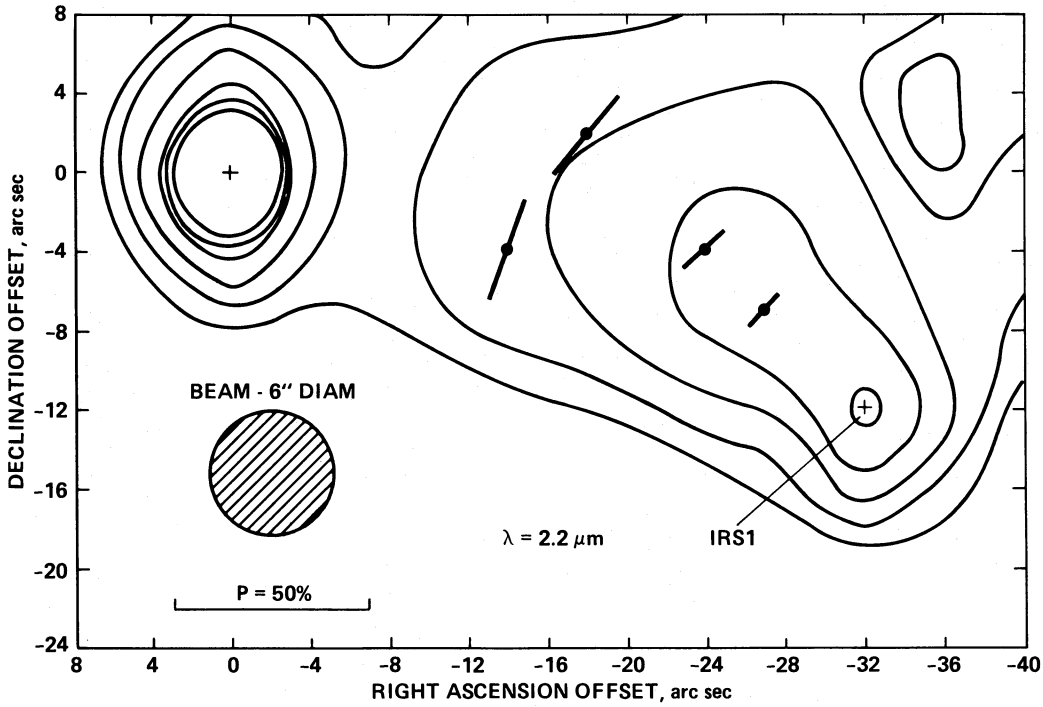

FIG. 3.—2.2 μm map of OMC-2/IRS 1, IRS 3, and the adjacent nebula made using a 6″ beam on a 4″ grid. Contour levels are 0.02, 0.03, 0.06, 0.13, 0.25, and 0.5 times the IRS 3 peak value of 0.67 Jy into a 6″ beam. Logarithmic contour levels were chosen to enhance the low-level surface brightness of the map. Polarization measurements made with a 6″ beam are shown on the map. The length of the heavy lines indicate the degree of polarization and their orientation gives the position angle of maximum electric vector. The pluses signify that the polarization measured at those points was less than 6% (3 σ). The coordinates are with respect to the IRS 3 position given in Table 1.

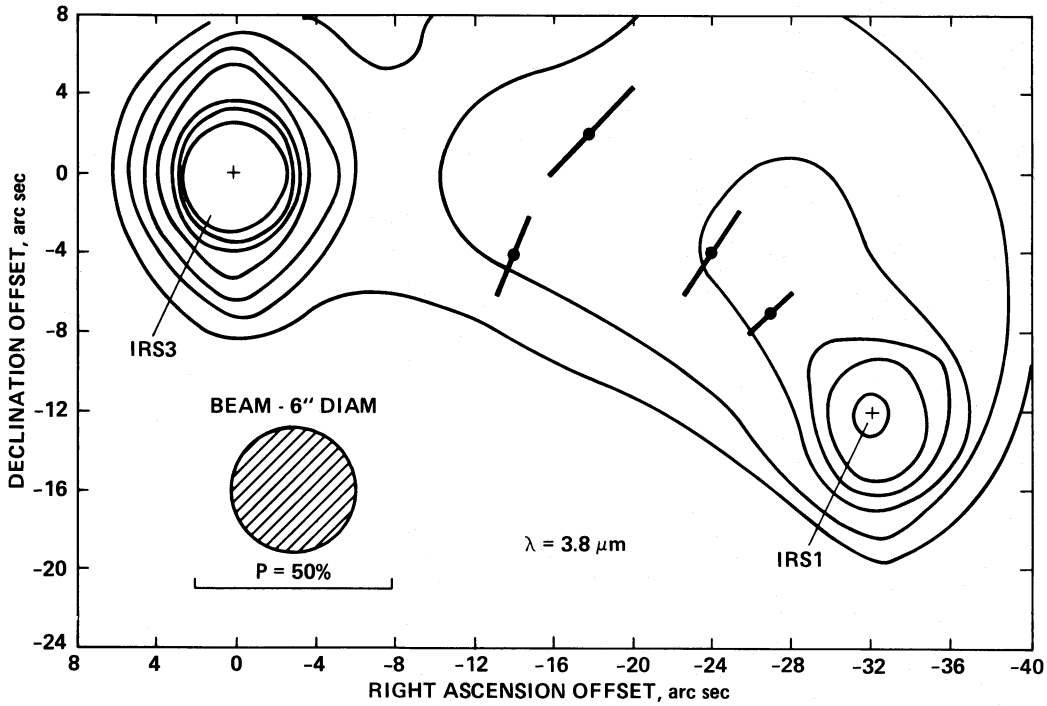

FIG. 4.—3.8 μm map of OMC-2/IRS 1, IRS 3, and the adjacent nebula made using a 6″ beam on a 4″ grid. Contour levels are 0.008, 0.02, 0.03, 0.06, 0.13, 0.25, and 0.5 times the IRS 3 peak value of 3.5 Jy into a 6″ beam; other features as in Fig. 3.

stein, and Capps 1983). The orientation of the electric vectors implies that IRS 1 is illuminating the grains. Surface brightness measurements, shown in Figure 5, along a northeast line extending radially outward from IRS 1 through the nebula show that the nebula is fairly uniform in brightness and color, and that the color is significantly bluer than that of IRS 1. All points in the nebula appear brighter than IRS 1 at the shortest wavelengths, showing that there is localized extinction along our direct line of sight to IRS 1. The 1.25–4.8 μm color temperature in the nebula is 1000 K or greater, too high to be attributable to thermal emission. Near-infrared continuum emission with color temperature in this range has been seen in visual reflection nebulae by Sellgren, Werner, and Dinerstein (1983), where it is associated with ultraviolet radiation and the 3.3 μm emission feature. Since neither of these appears to be present in OMC-2, we feel that it is unlikely that the (presumably nonequilibrium) processes producing the emission in visual reflection nebulae are occurring in OMC-2. Based on the high near-infrared color temperature and the high polarization, we therefore assume below that all the 1–5 μm radiation from the nebula is scattered light, even though we have polarimetry only at 2.2 and 3.8 μm.

The 3.05 μm absorption feature, attributed to ice, appears in the spectra of all points observed in the nebula as well as in the spectrum of IRS 1. The circular variable filter spectra of IRS 1 and a point in the nebula are shown in Figure 5*b*. Along the line of sight to IRS 1, the 3.05 μm feature has an optical depth of $\tau = 2$; and along the line of sight to a point in the nebula located 20″ from IRS 1, $\tau = 1.2$. The optical depths were derived by assuming a continuum level between 2.2 and 3.8 μm from the energy distributions shown in Figure 5. The continuum level was taken to be the intrinsic intensity $I_{\rm int}$, while the intensity measured in the depth of the ice band at 3.05 μm was taken to be the observed intensity $I_{\rm obs}$. Optical depths were derived from the relationship

$$I_{\rm obs}/I_{\rm int} = e^{-\tau_{3.05}} .$$

The higher optical depth toward IRS 1 supports our assertion that a large amount of localized extinction exists toward IRS 1. The 3.3 μm emission feature which appears in the spectra of visual reflection nebulae (Sellgren, Werner, and Dinerstein 1983) is not present in the spectrum of either IRS 1 or the nebula.

ii) IRS 3

Polarization measurements, given in Table 2, show that IRS 3 is not highly polarized. The 1–20 μm energy distribution for IRS 3 is shown in Figure 6. The total 1–20 μm luminosity is 50 $L_\odot$. Our results show that IRS 3 is a point source which peaks around 5 μm. The far-infrared data suggest that it is not a major luminosity source in the cloud.

iii) IRS 4

At 3.8 μm IRS 4 was resolved with a 4″ beam into two components, as shown in Figure 7. The components are separated by 4″ in the north-south direction and are referred to as IRS 4-N and IRS 4-S hereafter. IRS 4-N is highly polarized at 3.8 μm. A series of north-south scans through IRS 4 shown in Figure 8 reveals the interesting nature of IRS 4-N. It is comparably bright to IRS 4-S at 3.8 μm, but it is not seen as a discrete feature at either shorter or longer wavelengths until 20 μm, where it appears brighter than IRS 4-S. The importance of IRS 4-N at the longer wavelengths is further demonstrated by 30 μm observations with 4″ and 8″ apertures, which show that most of the flux from IRS 4 arises from a source centered on IRS 4-N. Comparison observations made of a point source, α Ori, and an extended object, BN, demonstrated that the flux

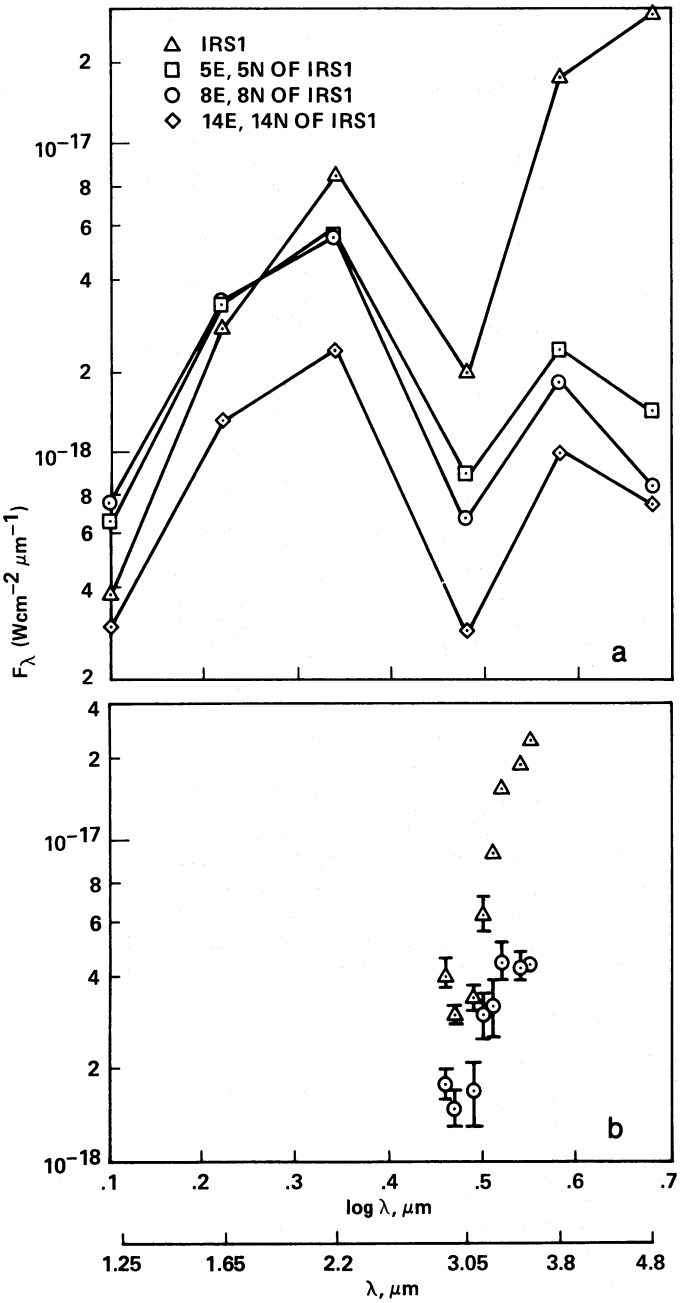

FIG. 5.—(*a*) 1.25–4.8 μm broad-band photometry energy distributions of IRS 1 and three positions in the nebula measured along a radial line through the nebula at points 5″, 8″, and 14″ east and north of IRS 1. (*b*) Circular variable filter measurements of IRS 1 and the 8″ east and north point in the nebula made from $2.8 \leq \lambda \leq 3.7$ μm using a 6″ beam.

from IRS 4-N originates from a region $\lesssim 4''$ in size. For this reason, we assume that the 50 μm and 100 μm radiation from IRS 4 is associated with IRS 4-N, which would then be the dominant luminosity source in the cluster. The 0.94 μm photograph published by Cohen and Frogel (1977) shows two components in the IRS 4 region. By comparison of their photograph to the star field visible in the guider at the IRTF, we determined that the northernmost component seen by those investigators coincides with the source we call IRS 4-S; IRS 4-N has not previously been identified.

IV. DISCUSSION

a) IRS 1 and the Adjacent Reflection Nebula

The classical method of dereddening the directly observed energy distribution fails badly in the case of OMC-2/IRS 1 because we do not know what to assume for the wavelength dependence of extinction in this region and because even with a 4″ aperture the flux observed directly from the position of IRS 1 includes contributions due to scattered light at wavelengths shorter than ~ 4 μm. We feel the simple arguments presented below demonstrate the usefulness of the scattered light as an alternate means of determining the nature of embedded objects. A similar approach has been used by Lenzen, Hodapp, and Solf (1984) in their analysis of Cep A.

i) Luminosity of IRS 1

The results of Thronson *et al.* (1978) show that the total luminosity of OMC-2 is no greater than $\sim 2100\ L_\odot$. Assuming that IRS 1 and IRS 4 make up the total luminosity, an estimate can be made of the luminosity of each. We scale the total luminosity according to the integrated flux into a 30″ beam at the peak positions. Since $L_{\rm IRS\,4}$ is ~ 3 times as bright as IRS 1, we assume that $L_{\rm IRS\,1} \leq 500\ L_\odot$. Our measurement of the total luminosity of OMC-2 is $\sim 900\ L_\odot$. Because the results of Thronson *et al.* show that the diffuse emission from outside the area mapped by us contributes significantly to the overall luminosity of the cloud, we feel that $500\ L_\odot$ is a reasonable upper limit for the luminosity of IRS 1.

ii) Temperature of IRS 1

The far-infrared results which show that IRS 1 is a primary luminosity source fit well with the near-infrared polarimetry at 2.2 and 3.8 μm, which clearly identifies IRS 1 as the illuminating source for the adjacent reflection nebula. We can use this circumstance to calculate the near-infrared blackbody temperature of IRS 1 by assuming that all the 1–5 μm radiation from the nebula is scattered light, and that IRS 1 is the sole illuminating source for the scattering grains. The scattered light from the nebula, together with the luminosity determined from the far-infrared observations, then provide a constraint on the temperature of IRS 1. This analysis is approximate but instructive. A more complete picture will result from detailed modeling of this region.

We have assumed isotropic scattering, that the nebular geometry is such that internal extinction and multiple scattering within the nebula can be neglected, that there is no reddening along our line of sight to the nebula, and that IRS 1 can be described as a blackbody of temperature T. The neglect of internal extinction is consistent with the uniformity of surface brightness and color of the nebula (Fig. 5). Knowing the luminosity of IRS 1 from the far-infrared observations, the flux which illuminates the nebula at each wavelength can be determined for any value of T, and the scattering probability in the 1–5 μm range can be calculated. The scattering probability $P(\lambda)$ is defined as the total flux scattered from a particular line of sight through the nebula divided by the illuminating flux reaching the grains along that line of sight:

$$P(\lambda) = \frac{F_\lambda(\text{neb})4\pi R^2}{L_*\langle F(\lambda, T)/\sigma T^4\rangle\langle\Omega/4\pi\rangle},$$

where F_λ(neb) is the nebular flux observed at wavelength λ, R is the distance to the source, L_* is the luminosity of the star, $F(\lambda, T)$ is the flux emitted from a blackbody of temperature T

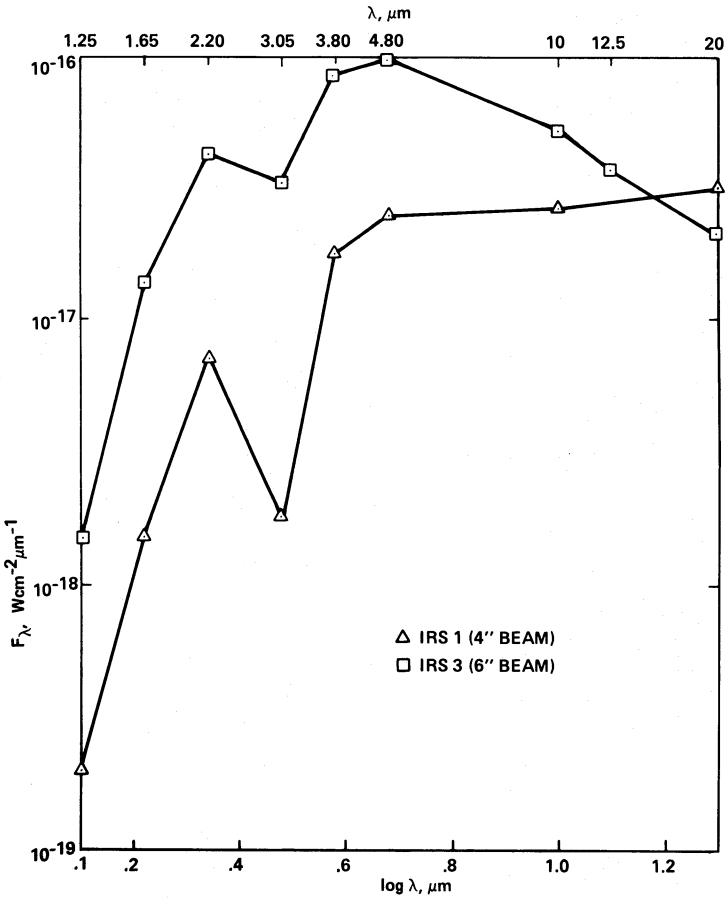

FIG. 6.—1.25–20 μm broad-band energy distributions of IRS 1 (4″ beam) and IRS 3 (6″ beam, $\lambda < 10$ μm; 4″ beam, $\lambda \geq 10$ μm)

at wavelength λ, σ is the Stephen-Boltzmann constant, and Ω is the solid angle subtended at the star by the portion of the nebula included in the beam. We analyze a position 14″ east and 14″ north of IRS 1, where the nebula was measured with a 6″ beam, so $\Omega \approx 0.3$ sr. We have taken L to be 500 $L_\odot$ and $R = 500$ pc.

Figure 9 displays $P(\lambda)$ for assumed temperatures of 850 and 1200 K for IRS 1. For $T \leq 850$ K, $P(\lambda)$ approaches unity at the shortest wavelengths. Since the probability cannot exceed unity, $T \leq 850$ K is not reasonable. At $T \geq 1200$ K, $P(\lambda)$ increases with wavelength at the longer wavelengths, which is inconsistent with general scattering theory for small particles with radius less than or equal to the wavelength. Applying the constraints on $P(\lambda)$ that it not exceed unity at any wavelength and that it decrease with increasing wavelength, this simplified model of IRS 1 and the adjacent nebula suggests that IRS 1 is at a temperature of ~ 1000 K. We note that this conclusion is based on the wavelength dependence as well as the absolute value of $P(\lambda)$. Although extinction within the nebula or along the line of sight could affect the results somewhat, large amounts of extinction would be required to produce significant changes in the color of the scattered light and thus in the range of plausible temperatures. However, introducing more than a few magnitudes of extinction results in $P(\lambda)$ coming implausibly near unity. Thus, to the extent that the near-infrared energy distribution of the illuminating radiation from IRS 1 can be described by a single blackbody temperature, we feel that the temperature must be close to 1000 K. The amount of extinction implied by matching the assumed physical properties of IRS 1 ($L \approx 500$ $L_\odot$, $T = 1000$ K) with our direct near-infrared observations of IRS 1 is ~ 3.5 mag at 4.8 μm; this wavelength is chosen as being least affected by scattering or thermal emission. Assuming $\tau(\lambda)$ varies as $\lambda^{-1.45}$ (Becklin *et al.* 1978) gives $A_v \approx 75$ along the line of sight to IRS 1; alternatively, the extinction law derived by Rieke and Lebofsky (1985) suggest $A_v \approx 85$–90. This estimate of the extinction refers only to the direct line of sight to the illuminating object, IRS 1, which is known from the scattered light data to pass through localized extinction. Thus, the estimate derived here can be reconciled with the lower value, $A_v \approx 15$, derived from the far-infrared optical depth averaged over a 30″ field of view including IRS 1.

Because IRS 1 is an infrared source, the far-infrared emitting grains in the IRS 1 nebula must be heated at infrared wavelengths. A comparison with the visual reflection nebula NGC 7023 studied by Whitcomb *et al.* (1981) demonstrates that this is plausible. In NGC 7023, the heating flux (emitted primarily at ~ 2000 Å) received by a grain at a projected distance of 0.2 pc from the central star is 3.5×10^{-7} W cm^{-2}. In the OMC-2/IRS 1 nebula the same amount of flux is received by a grain located 30″ from IRS 1, which corresponds to a projected distance of 0.07 pc. The dust grain temperatures at the aforementioned positions are 55 K in the NGC 7023 nebula and 29 K in the OMC-2/IRS 1 nebula, even though the grains receive the same amount of flux. The lower dust temperature in the IRS 1 nebula can be understood qualitatively if the grains are heated at infrared wavelengths, since grains absorb less efficiently in

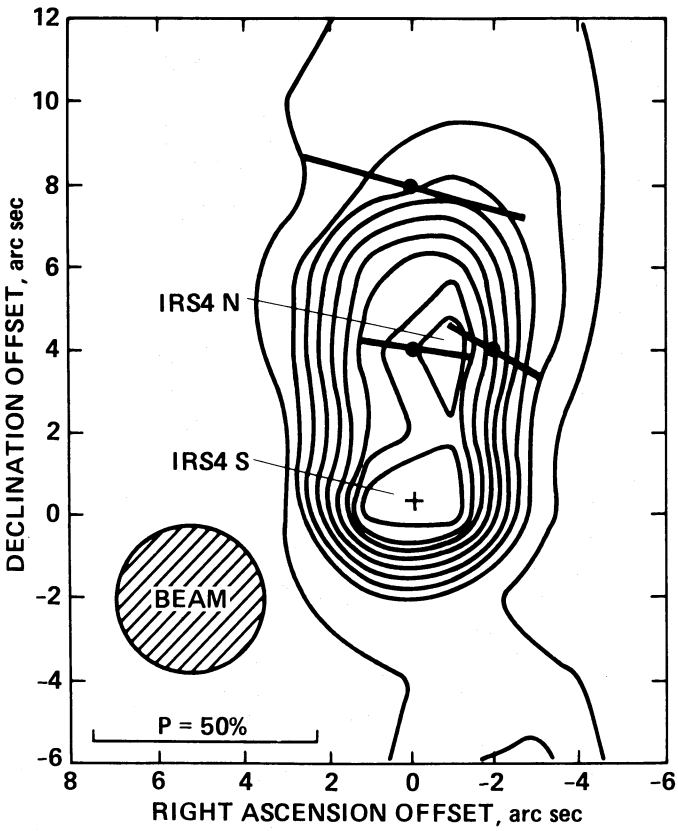

FIG. 7.—3.8 μm photometric map of IRS 4-N and IRS 4-S made using a 4″ beam on a 2″ grid. Contour levels are 0.1, 0.2, 0.3, 0.4, 0.5, 0.6, 0.7, 0.8, and 0.9 times the IRS 4-S peak value of 0.3 Jy into a 4″ beam. Polarization measurements made with a 4″ beam are shown on the map. The length of the heavy lines indicate the degree of polarization, while their orientation gives the position angle of the maximum electric vector. The plus signifies that the polarization measured at that point was less than 6% (3 σ). The co-ordinates are with respect to the IRS 4-S position given in Table 1.

the infrared than in the ultraviolet. A similar conclusion is reached if half the 100 μm flux at the position 30″ from IRS 1 is attributed to material elsewhere along the line of sight heated by IRS 4.

To summarize, our data suggest that IRS 1 is an object with $T \approx 1000$ K and $L \leq 500\ L_\odot$. Our direct view of it is obscured by localized extinction, while the grains in the nebula are illuminated by IRS 1 with little intervening extinction. Several possibilities exist as to the nature of IRS 1. It could be a fairly mature star embedded in a circumstellar shell which radiates at 1000 K. It is perhaps more satisfying to assume that IRS 1 is a younger object, so that 1000 K is the temperature of the collapsing envelope of a protostar. Under this asssumption, comparison with published protostellar tracks (Larson 1972) shows that the inferred luminosity and temperature are characteristic of a 3–5 $M_\odot$ object $\sim 10^6$ yr after the onset of collapse.

iii) Grain Properties

For $T \approx 1000$ K and $L = 500\ L_\odot$, we find $P \approx 0.05$ as an average value between 1 and 5 μm (Fig. 9). The neglect of extinction along the scattering path, and the fact that L may be less than 500 $L_\odot$ for IRS 1, underestimate P. The scattering probability is related to the grain albedo ω as

$$P = \tau(\text{neb})\omega\ ,$$

where τ(neb) is the optical depth to the illuminating radiation along a ray through the region of the nebula within the observing beam. Because $\tau(\text{neb}) \leq 1$, we have $\omega \geq P$. A more straightforward way to estimate ω, which is independent of specific assumptions about the illuminating source, is to calculate the albedo by comparing the intensity of the scattered 1–5 μm light and the intensity of the far-infrared radiation. The similarity of

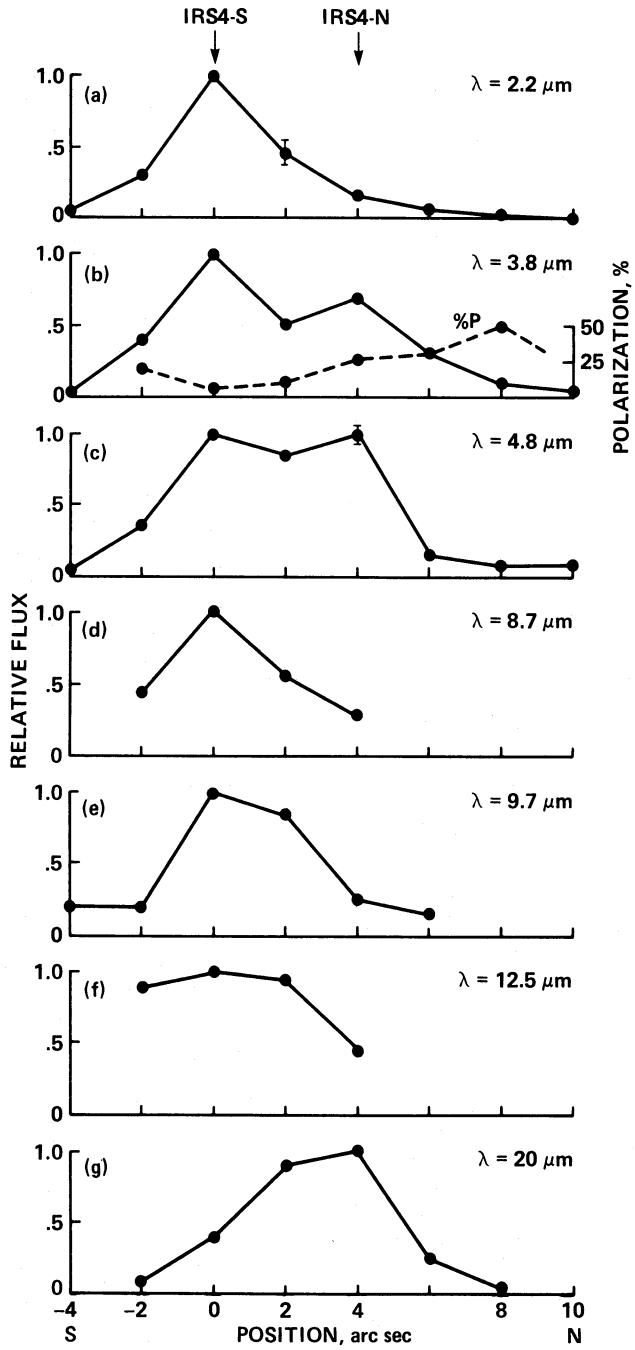

FIG. 8.—North-south photometric scans through IRS 4 at λ = 2.2, 3.8, 4.8, 8.7, 9.7, 12.5, and 20 μm, using a 4″ beam, which show the relative flux of IRS 4-N and IRS 4-S. A polarization scan at 3.8 μm is superposed on the 3.8 μm flux scan. The scan was constructed from scans made with the wire grid fixed at position angles of 90° and 0°, assuming a polarization position angle of 90° at all points along this line, as suggested by Fig. 7.

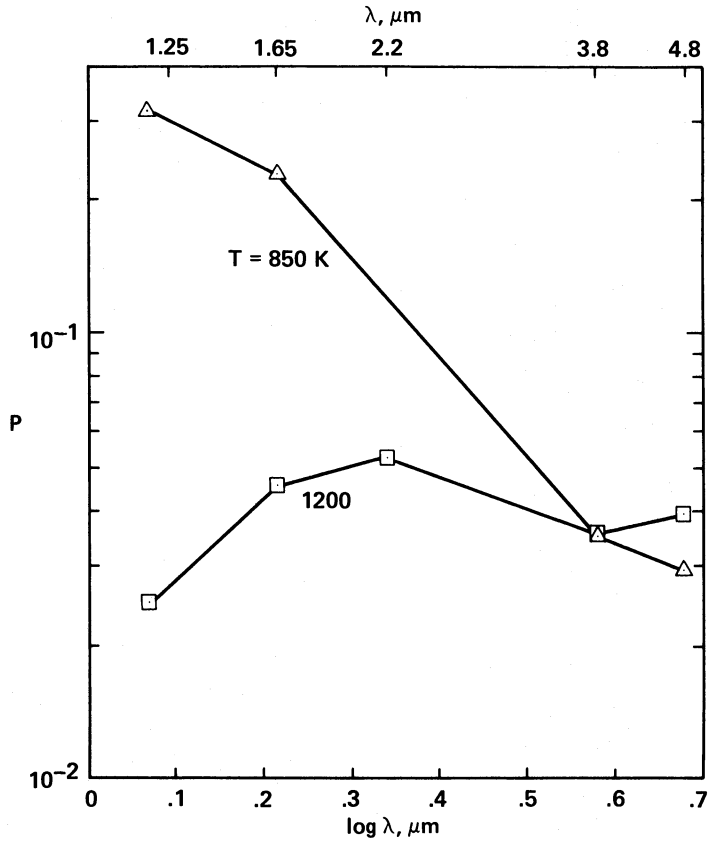

FIG. 9.—The near-infrared scattering probability P as defined in the text is shown for intrinsic temperature values for IRS 1 of 850 K and 1250 K.

the 100 μm and 2.2 μm dust distribution and the fact that IRS 1 is heating grains at near-infrared wavelengths imply that the dust which scatters light in the near-infrared is also radiating at 100 μm, and that it is heated by the near-infrared radiation which it absorbs rather than scatters. Because

$$\omega = \sigma(\text{scat})/\langle\sigma(\text{scat}) + \sigma(\text{abs})\rangle ,$$

where σ(scat) is the scattering cross section and σ(abs) is the absorption cross section, we can estimate the near-infrared albedo of the dust in the IRS 1 nebula by taking σ(scat) proportional to B(scat), the surface brightness of the 1–5 μm flux, and σ(abs) proportional to B(abs), the luminosity integrated over wavelength from the 50 and 100 μm measurements. Thus,

$$\omega \approx B(\text{scat})/\langle B(\text{scat}) + B(\text{abs})\rangle .$$

The point in the nebula used for this calculation is located 20″ northeast of IRS 1. The quantities B(abs) = 5.5×10^{-8} W cm^{-2} sr^{-1} and B(scat) = 4.6×10^{-9} W cm^{-2} sr^{-1} at this point. We find $\omega = 0.08$ as an average value from 1 to 5 μm in this fashion. The 100 μm map (Fig. 2) shows that grains heated by IRS 4 may contribute to the flux from the IRS 1/nebula region. If so, this calculation underestimates the albedo. We also have neglected the effects of multiple scattering and internal extinction, both of which would also serve to make the albedo, as calculated above, less than the true albedo. Therefore, 0.08 should be considered a lower limit to the true grain albedo. A comparison of our result for grain albedos in the near-infrared to standard grain models (Draine and Lee 1984) reveals that a mixture of graphite and silicate grains in a Mathis, Rumpl, and Nordsieck (1977) size distribution could have the near-infrared albedo 0.08 or greater required by the data.

iv) Polarimetry and Spectrophotometry

The percent polarization increases with distance from the source at both 2.2 and 3.8 μm. Although the polarization measured near the source will be diluted by the variation of scattering angles across the beam, this effect can account for no more than 10% of the increase in polarization we observe. Another possibility is that the effect is due to the geometry of the IRS 1 nebula. If the scattering angle is closer to 90° at larger distances from the source, it may account for the higher polarization seen at those points. We note that the polarization is larger at 3.8 μm than at 2.2 μm, a trend that increases close to the source. This may imply that the effects of multiple scattering must be included in any comprehensive model of this region. The wavelength and spatial variation of polarization will be investigated through further modeling.

The absence of the 3.3 μm emission feature which appears in the spectra of visual reflection nebulae indicates that the mechanism which excites this feature is not present in OMC-2. This is consistent with the idea put forth by Sellgren (1984) that the absorption of ultraviolet photons by small grains or large molecules produces the 3.3 μm feature by a nonequilibrium process. There are no ultraviolet photons available to produce this feature in the IRS 1 nebula because the illuminating star is an infrared source.

The 3.1 μm ice band absorption feature appears in the spectra of both the illuminating source and the reflection nebula. It is not clear whether the feature originates in a dust shell surrounding IRS 1, in the nebula, or in line-of-sight

material. A correlation has been observed between the depth of the 3.1 μm absorption feature and high polarization in star formation regions (Joyce and Simon 1982). These authors suggest that metallic oxide grain cores surrounded by icy mantles are responsible for this correlation. In their model the ice absorption is produced by the mantles, while the polarization is a result of grain alignment in a magnetic field, which may be enhanced by the paramagnetic properties of the mantle (Duley 1978). This model may apply to objects such as the BN object, where dichroic absorption is responsible for the polarization. In the case of OMC-2/IRS 1, however, our observations which show both high polarization due to scattering and an ice band in the spectrum of the nebula suggest that a geometrical explanation for this correlation is likely. Consider a source with the general character of OMC-2/IRS 1 observed from two angles (Fig. 10). An observer with an obscured view of the star sees high polarization and a deep ice band. This corresponds to our view of OMC-2/IRS 1. An observer looking in from an orthogonal direction will see the central object more clearly and much lower polarization, because of symmetry and because a much smaller fraction of the light is scattered. The observer will also see a weaker ice band (see Fig. 10). If this geometrical effect is in fact the correct explanation for the Joyce-Simon correlation, it implies that the ice band may not be present in the intrinsic spectrum of the source which illuminates the reflection nebula in OMC-2 or in similar objects. It is interesting to examine what the OMC-2/IRS 1 region would look like if it were at a distance such that it could not be spatially resolved. We calculate the percent polarization, averaged over the IRS 1 nebula, to be 13% at 2.2 μm, while the optical depth of the ice band is $\tau = 1.2$. The source would then appear similar to those objects cited by Joyce and Simon as having deep ice bands and high polarization. Note that other reflection nebulae show ice-band absorption (Cep A, Lenzen, Hodapp, and Solf 1984; NGC 6334, Simon *et al.* 1985). These objects, like OMC-2/IRS 1, have both deep ice bands and high polarization. In each case it is clear that the principal polarization mechanism is scattering rather than dichroic absorption.

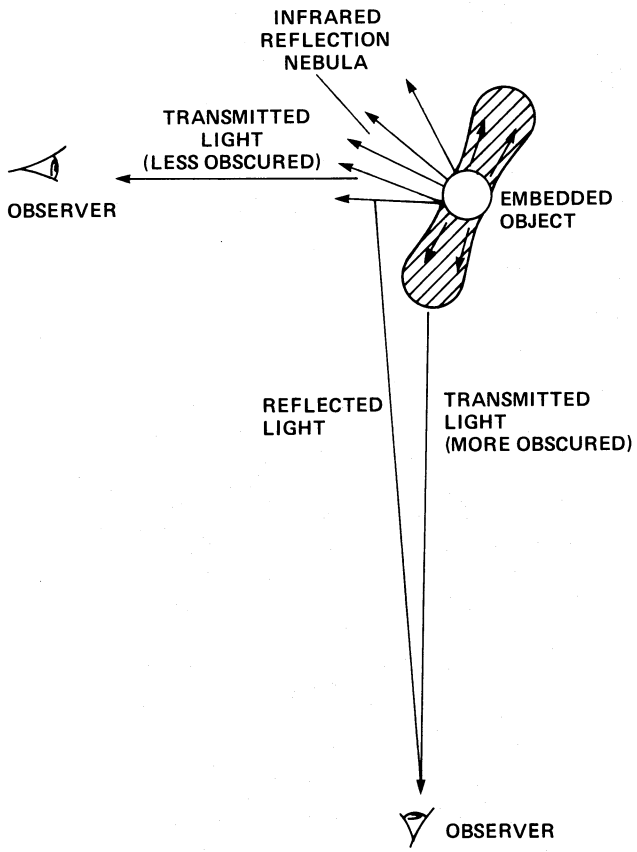

FIG. 10.—A schematic diagram of the IRS 1 nebula and the embedded protostar as seen from orthogonal directions.

b) The IRS 3 Region

Unlike the cases of IRS 1 and IRS 4, the flux from IRS 3 peaks in the near-infrared. The absence of appreciable far-infrared emission suggests that IRS 3 is not a prime luminosity source within the cloud and indicates that our view of IRS 3 is not influenced by large amounts of extinction local to the source. The weak ice band observed toward IRS 3 is consistent with this picture. The absence of associated strong far-infrared emission makes OMC-2/IRS 3 rather unusual among embedded infrared sources; perhaps complex geometries and dust distributions like that sketched in Figure 10 are common, so that only in rare cases does one get a direct view of the central star or protostar. One could then refer to OMC-2/IRS 3 as a "naked protostar." An alternative possibility is that IRS 3 is a background object viewed through the cloud.

c) The IRS 4 Region

The two components of IRS 4 exhibit unusual phenomonology (Fig. 8). The northern component, IRS 4-N, is comparably bright to the southern component IRS 4-S at 3.8 μm and 4.8 μm but is not seen at longer wavelengths until 20 μm. From the 3.8 μm polarimetry, IRS 4-N appears to be an infrared reflection nebula which is illuminated by IRS 4-S. The absence of IRS 4-N at 8.7, 9.7, and 12.5 μm is understandable under this picture, since scattering is less efficient at longer wavelengths. The continuity of the polarization with position shown in Figure 8*b* argues against the possibility that IRS 4-N is a background source seen at 2.2 and 3.8 μm through polarized foreground scattered light. However, at 20 μm and 30 μm IRS 4-N is the dominant member of the pair and indeed the most luminous object in OMC-2. Clearly, two phenomena, a luminous far-infrared source and a near-infrared reflection nebula, are both located along the line of sight to IRS 4-N. It is logical to attribute these phenomena to a single object. One intriguing possibility is that the scattering at 3.8 μm is due to an extended envelope or dust shell which surrounds IRS 4-N and is illuminated at short wavelengths by IRS 4-S. In detail we have found it difficult to make this model work, basically because IRS 4-N is much fainter than IRS 4-S at 2.2 μm. The other possibility is that IRS 4-N itself is responsible for illuminating a very compact, very local reflection nebula at short wavelengths. In this case, the orthogonality of the polarization position angles to the direction toward IRS 4-S is merely concidental. Further work, perhaps at very high spatial resolution, will be required to improve our understanding of this peculiar pair of objects.

d) Comparison of Infrared and Visible Reflection Nebulae

Ultraviolet and visual observations of reflection nebulae such as NGC 7023 and the Pleiades have been one of the main means of obtaining data on the properties of interstellar grains at these wavelengths (Witt *et al.* 1982). Sellgren, Werner, and Dinerstein (1983) extended the data on this class of objects to

longer wavelengths but found the infrared emission to be dominated by nonequilibrium processes whose nature is still uncertain (Sellgren 1984; Sellgren *et al.* 1985). Thus, classical visual reflection nebulae illuminated by early-type stars are not good sites for the study of the infrared properties of the bulk of the interstellar grains. It now appears that such information may be obtainable through the study of infrared reflection nebulae, such as OMC-2, which are illuminated by infrared sources. The brightness of the scattered infrared radiation can be quite high for present techniques, and the absence of ultraviolet radiation suppresses the nonequilibrium infrared emission seen in the visual nebulae. In subsequent papers, we will construct models of infrared reflection nebulae to determine the constraints which observations such as these place upon the properties of interstellar grains.

V. CONCLUSIONS

We have carried out an extensive program of polarization, photometry, and spectrophotometry of the OMC-2 cluster at infrared wavelengths from 1 to 100 μm. We find that the point sources in the cluster are embedded in a complex and inhomogeneous distribution of dust clouds which strongly modify our view of them. The results highlight the prevalence of 1–5 μm reflection nebulae in regions of star formation and the consequent importance of polarimetry as a probe of such regions. We have identified the OMC-2/IRS 1 nebula as a particularly good example of an infrared reflection nebula that is well suited to further observational and theoretical study. In conclusion, our results show that:

1. The compact sources IRS 1 and IRS 4 are the main luminosity sources in the OMC-2 region. IRS 1 illuminates the grains in the adjacent reflection nebula; IRS 4 has double source structure; and IRS 3, the brightest object in the region at $\lambda \leq 10$ μm, is not an important luminosity source.

2. The reflected light from the IRS 1 nebula provides additional constraints on and information about the illuminating source that cannot be obtained through direct line-of-sight observations. The analysis of the scattered light and the constraints from the far-infrared observations show that OMC-2/IRS 1 can be characterized by $L \leq 500\ L_{\odot}$ and $T \approx 1000$ K. If IRS 1 is a protostar with $L \approx 500\ L_{\odot}$, and $T \approx 1000$ K, then it corresponds to a 3–5 $M_{\odot}$ object at an age of $\sim 10^6$ yr following the onset of collapse.

3. The near-infrared (1-5 μm) albedo of the grains in the nebula is $\omega \geq 0.08$.

We thank Harriet Dinerstein, Paul Harvey, Marshall Joy, Charlie Kaminski, Kris Sellgren, and Xander Tielens for assistance with the observations. We appreciate the support of the staffs of the Kuiper Airborne Observatory and the NASA Infrared Telescope Facility. We are grateful to Xander Tielens, Mike Castelaz, Lou Allamandola, Dick Miller, David Rank, and Peter Bodenheimer for helpful discussions. We also thank an anonymous referee for helpful comments and suggestions. The work at Ames has been supported by the Astrophysics Division of NASA, and the work at Texas by NASA grant NAG2-67.

REFERENCES

Batrla, W., Wilson, T. L., Bastien, P., and Ruf, K. 1983, *Astr. Ap.*, **128**, 279.
Becklin, E. E., Matthews, K., Neugebauer, G., and Willner, S. P. 1978, *Ap. J.*, **220**, 831.
Cohen, J. G., and Frogel, J. 1977, *Ap. J.*, **211**, 178.
Draine, B. T., and Lee, H. M. 1984, *Ap. J.*, **285**, 89.
Duley, W. W. 1978, *Ap. J. (Letters)*, **219**, L129.
Dyck, H. M., and Lonsdale, C. J. 1981, in *Infrared Astronomy*, ed. C. G. Wynn-Williams and D. P. Cruikshank (Dordrecht: Reidel), p. 223.
Gatley, I., Becklin, E. E., Matthews, K., Neugebauer, G., Penston, M. V., and Scoville, N. 1974, *Ap. J. (Letters)*, **191**, L121.
Harvey, P. 1979, *Pub. A.S.P.*, **91**, 143.
Harvey, P., Wilking, B., and Joy, M. 1984, *Nature*, **307**, 441.
Joyce, R. R., and Simon, T. 1982, *Ap. J.*, **260**, 604.
———. 1986, *A.J.*, **91**, 113.
Kutner, M. L., Evans, N. J., II, and Tucker, K. D. 1976, *Ap. J.*, **209**, 452.
Larson, R. B. 1972, *M.N.R.A.S.*, **157**, 121.
Lenzen, R., Hodapp, K.-W., and Solf, J. 1984, *Astr. Ap.*, **137**, 202.
Mathis, J. S., Rumpl, W., and Nordsieck, K. H. 1977, *Ap. J.*, **217**, 425.
Rieke, G., and Lebofsky, M. 1985, *Ap. J.*, **288**, 618.
Savage, B. D., and Mathis, J. S. 1979, *Ann. Rev. Astr. Ap.*, **17**, 73.
Sellgren, K. 1984, *Ap. J.*, **277**, 623.
Sellgren, K., Allamandola, L. J., Bregman, J. D., Werner, M. W., and Wooden, D. H. 1985, *Ap. J.*, **299**, 416.
Sellgren, K., Werner, M., and Dinerstein, H. 1983, *Ap. J. (Letters)*, **271**, L13.
Simon, T., Dyck, H. M., Wolstencroft, R. D., Joyce, R. R., Johnson, P. E., and McLean, I. S. 1985, *M.N.R.A.S.*, **212**, 21P.
Thronson, H. A., Harper, D. A., Keene, J., Loewenstein, R. F., Moseley, H., and Telesco, C. M. 1978, *A.J.*, **83**, 492.
Tokunaga, A. T., Lebofsky, M. J., and Rieke, G. H. 1981, *Astr. Ap.*, **99**, 108.
Werner, M. W., Dinerstein, H. L., and Capps, R. W. 1983, *Ap. J. (Letters)*, **265**, L13.
Whitcomb, S. E., Gatley, I., Hildebrand, R. H., Keene, J., Sellgren, K., and Werner, M. W. 1981, *Ap. J.*, **246**, 416.
Wilking, B. A., Harvey, P. M., Lada, C. J., Joy, M., and Doering, C. R. 1984, *Ap. J.*, **279**, 291.
Witt, A. N., Walker, G. A. H., Bohlin, R. C., and Stecher, T. P. 1982, *Ap. J.*, **261**, 492.

R. W. CAPPS: Institute for Astronomy, University of Hawaii, 2680 Woodlawn Dr., Honolulu, HI 96822

D. F. LESTER: Department of Astronomy, University of Texas, RLM Hall 15.308, Austin, TX 78712

Y. PENDLETON and M. W. WERNER: NASA/Ames Research Center, Mail Stop 245-6, Moffett Field, CA 94035